When Is a Helix Stable?

Andy Borum*
Department of Mathematics, Cornell University, Ithaca, New York 14853, USA

Timothy Bretl†
Department of Aerospace Engineering, University of Illinois at Urbana-Champaign, Urbana, Illinois 61801, USA

(Received 22 June 2020; accepted 17 July 2020; published 20 August 2020)

We determine which helical equilibria of an isotropic Kirchhoff elastic rod with clamped ends are stable and which are unstable. Although the set of all helical equilibria is parametrized by four variables, with an additional fifth parameter determined by the rod's material, we show that only three of these five parameters are needed to distinguish between stable and unstable equilibria. We also show that the closure of the set of stable equilibria is star convex. With these results, we are able to compute and visualize the boundary between stable and unstable helices for the first time.

DOI: 10.1103/PhysRevLett.125.088001

Introduction.—In 1859, Kirchhoff observed that the centerline of an inextensible, unshearable, isotropic, and uniform elastic rod in equilibrium can be a circular helix, and he classified all helical equilibria for rods of this type [1,2]. This classification was extended to rods that are extensible and shearable, but still isotropic and uniform, by Antman [3] and Whitman and DeSilva [4], and the extension to anisotropic rods was later completed by Chouaieb, Goriely, and Maddocks [5–7]. A natural question to ask is which of these helical equilibria are stable, i.e., which helices locally minimize elastic potential energy, in an appropriate sense. A complete answer to this question has not been obtained before now. In this Letter, we determine which helical equilibria of an inextensible, unshearable, isotropic, and uniform elastic rod with clamped ends are stable and which are unstable.

There has been considerable work on analyzing the stability of elastic rods in both helical and more general configurations, with two approaches taken in previous literature. First, dynamical methods can be used to determine how perturbations to an equilibrium configuration grow in time [8–18]. Second, potential energy methods can be used to determine if an equilibrium configuration is a local minimum of an elastic energy functional among an appropriate class of perturbations [5,19–32]. (See [5,12–23,28,30] for work pertaining to rods with helical centerlines and [24–27,31] for work on the degenerate case of a helical rod with a straight or circular centerline.) In this Letter, we focus on the potential energy method, but we note that the relationship between dynamical and potential energy methods is not fully understood ([33], Chap. 5.7).

When using the potential energy method, approaches to determining if an equilibrium configuration locally minimizes elastic energy include the use of integral inequalities [19–25], bifurcation methods [5,26–29], and the conjugate point test from the calculus of variations [5,29–32]. Various boundary conditions at the ends of the rod can be considered when using the above methods to determine stability, including clamped ends, loaded ends, or mixed boundary conditions (although the application of the conjugate point test with nonclamped ends is a delicate issue [34,35]). In this Letter, we use the conjugate point test and consider the case of clamped ends.

None of the approaches described above have so far provided analytical conditions for stability that apply to all helical rods. Analytical conditions based on integral inequalities are typically only necessary or sufficient for stability. Conditions based on dynamical, bifurcation, and conjugate point methods can be evaluated analytical only for special types of helices, e.g., rods with circular centerlines. For this reason, numerical computation (using one of these methods) has so far been the only way to determine if an arbitrary helical rod is stable.

In principle, anyone could have used numerical computation to compute—exhaustively—the set of all stable helical equilibria before now. However, for an inextensible, unshearable, isotropic, and uniform elastic rod, the set of all equilibrium configurations with helical centerlines is parametrized by four variables [5–7], and changing the rod's material introduces a fifth parameter. The results of exhaustive computation in this five-dimensional parameter space would have been difficult to visualize and would have provided little qualitative insight.

In this Letter and a companion paper [36], we derive several invariance and scaling properties that simplify the process of distinguishing between stable and unstable helical equilibria using the conjugate point method. We show that only three of the five parameters described above are needed to determine the stability of a helical rod, and we show that the closure of the set of stable helical rods—a

subset of this reduced, three-dimensional parameter space—is star convex. This geometric result allows us to compute points on the boundary between stable and unstable helices by sampling a hemisphere. As a consequence, we can compute and visualize the boundary between stable and unstable sets of helical equilibria. This visualization leads to a new result, that a helical rod of length L with curvature less than $2\pi/L$ and with arbitrary torsion is stable if it is sufficiently twisted.

Equilibrium and stability.—We begin by describing conditions for equilibrium and stability of elastic rods. We note that conditions for stability based on the conjugate point test have previously been derived using a Lagrangian formulation [5,29–32] and were used to numerically analyze the stability of elastic rods with helical centerlines [5,30]. The approach used in this Letter, however, is based on a Hamiltonian formulation of the conjugate point test [37], which allows us to derive several properties of conjugate points in helical rods.

The configuration of an inextensible and unshearable rod of length L is described by the maps $r:[0,L]\to\mathbb{R}^3$ and $R:[0,L]\to SO(3)$, where $SO(3)$ is the set of three-dimensional rotation matrices. The map r describes the rod's centerline, and R describes the orientation of a triad of orthonormal vectors attached to the rod's centerline [33]. These functions must satisfy

$$r' = Rv \qquad R' = R\hat{u}, \tag{1}$$

where primes denote differentiation with respect to arc length $s\in[0,L]$, $v=[1\quad 0\quad 0]^T$, and the map $\hat{}:\mathbb{R}^3\to\mathfrak{so}(3)$ satisfies $a\times b=\hat{a}b$ for all $a,\ b\in\mathbb{R}^3$. The first element u_1 of the vector u is the twisting strain, and the second and third elements u_2 and u_3 are the bending strains. We enforce clamped boundary conditions on the positions $r(0), r(L)$ and orientations $R(0), R(L)$ at the rod's ends.

The elastic energy of an isotropic elastic rod is

$$\frac{1}{2}\int_0^L (cu_1^2+u_2^2+u_3^2)ds, \tag{2}$$

where $c>0$ is the ratio of torsional to bending stiffness. We assume the rod is uniform so that c is constant. The conditions for a configuration of the rod to be in equilibrium [i.e., to be an extremal of the energy (2)] are that, in addition to satisfying (1) and the boundary conditions, there exist functions $m,\ n:[0,L]\to\mathbb{R}^3$ satisfying

$$\begin{aligned} &m' = m\times u + n\times v, \quad && n' = n\times u, \\ &u_1 = c^{-1}m_1, && u_2 = m_2, \qquad u_3 = m_3. \end{aligned} \tag{3}$$

Mechanically, the functions m and n describe the internal moments and forces, respectively, acting on the rod [33]. In the Hamiltonian formulation, m and n are adjoint variables associated with the constraints (1) [37,38].

We say that a rod is helical if its centerline r is a circular helix, i.e., its curvature and torsion are constant. Solutions of the system (3) corresponding to helical centerlines with curvature $\kappa\geq 0$ and torsion τ have the form

$$m(s)=\begin{bmatrix}\omega\\ \kappa\cos(\gamma s+\phi)\\ \kappa\sin(\gamma s+\phi)\end{bmatrix} \qquad n(s)=(\omega-\tau)\begin{bmatrix}\tau\\ m_2(s)\\ m_3(s)\end{bmatrix}, \tag{4}$$

where ω is the twisting moment, ϕ is a phase parameter, and $\gamma=\tau-\omega/c$ [cf. Ref. [6], Eqs. (86) and (94); Ref. [12], Eqs. (4.6)–(4.9)].

For a given equilibrium configuration of the rod, the conjugate point condition can be applied to determine if the configuration locally minimizes the elastic energy functional (2) [5,29–32]. To apply the conjugate point test, Eqs. (1) and (3) are linearized, resulting in a linear system of the form

$$J' = HJ+GM, \qquad M' = FM, \tag{5}$$

where F, G, and H are 6×6 matrices that depend on m, n, and c. (Expressions for F, G, and H are given in the companion paper [36].) The system (5) is solved with the initial conditions $J(0)=0_{6\times 6}$ and $M(0)=I_{6\times 6}$, where $0_{6\times 6}$ is the 6×6 matrix containing all zeros and $I_{6\times 6}$ is the 6×6 identity matrix. If $\det[J(s)]=0$ for some $s\in(0,L)$, then s corresponds to a conjugate point and the equilibrium configuration is not stable. If $\det[J(s)]\neq 0$ for all $s\in(0,L]$, then there are no conjugate points and the equilibrium configuration is stable [37].

The conjugate point test can be applied to the helical rod solutions in (4) for any values of $\kappa>0$, τ, ω, ϕ, and $c>0$. The test cannot be applied, however, when $\kappa=0$, which corresponds to a straight, twisted rod. Because of the clamped boundary conditions and the assumption of inextensibility, the straight, twisted rod is an isolated configuration (i.e., there are no nearby admissible configurations with nonstraight centerlines), and is therefore an abnormal extremal of the elastic energy (2) [37].

Reduction of the parameter space.—Five parameters appear in the expressions (4) corresponding to helical rods. Four of these parameters, κ, τ, ω, and ϕ, describe the helical configurations of the rod (cf. [5–7]), while the fifth parameter c depends upon the rod's material properties. We now show that only three of these parameters, κ, τ, and ω, are needed to distinguish between stable and unstable helical rods. As one might expect, the phase ϕ does not affect stability. This invariance results from the isotropy of the rod, and changing ϕ simply corresponds to rotating the reference frame in which equations (3) are written. In the companion paper [36], we show that a coordinate transformation can be used to remove the dependence upon ϕ in the system (5).

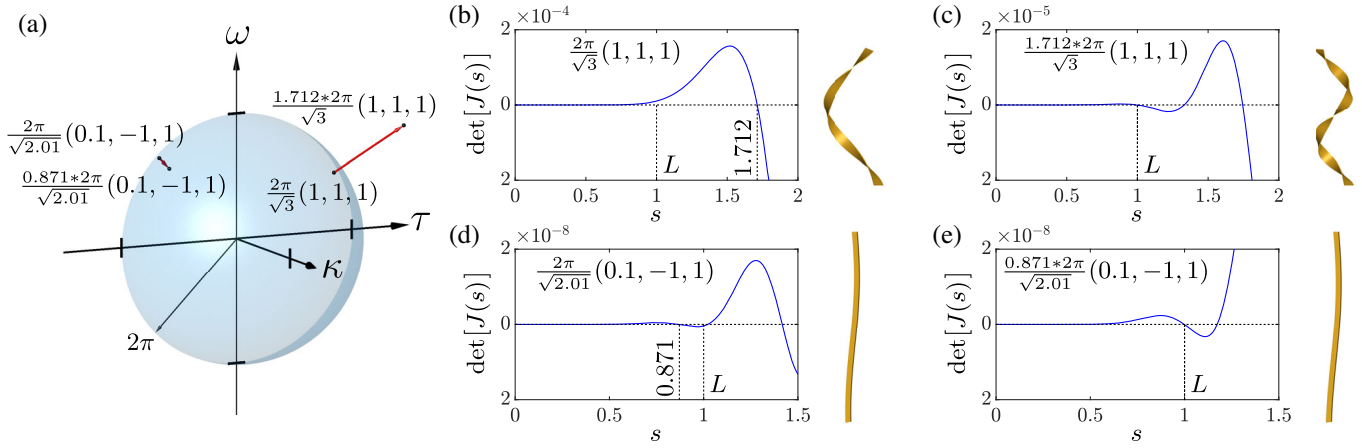

FIG. 1. A procedure for computing the boundary between stable and unstable helical rods in the κ-τ-ω parameter space. Each ray extending from the origin intersects the boundary exactly once. This intersection is found by selecting a point (κ, τ, ω) on the ray, computing the first conjugate point $s_c(\kappa, \tau, \omega)$, and scaling the point by $s_c(\kappa, \tau, \omega)/L$. The entire boundary can be found by repeating this procedure for all points on a hemisphere of radius 2π. Two examples of this procedure are shown in Fig. 2(a) for $L = 1$. Figures 2(b)–2(e) show plots of $\det[J(s)]$ at each of the four points in Fig. 2(a), which are used to find $s_c(\kappa, \tau, \omega)$. Also shown are the corresponding helical rod configurations. Although we consider isotropic rods, the depicted rods are drawn as ribbons to show the rod's twist.

Less apparent, however, is the invariance of stability under changes in the stiffness parameter c. If κ, τ, and ω are fixed in (4), varying c has no effect on the rod's centerline, which has curvature κ and torsion τ. Varying c does, however, affect the twist u_1 as shown in (3). Varying c also changes the weight placed on twist in the elastic energy functional (2). Together, the changes in twist and in twist energy result in no change in stability. In the companion paper [36], this property is established by integrating (5) to find a closed-form expression for $J(s)$ and then showing that varying c does not affect the arc lengths at which $\det[J(s)] = 0$. Note that if τ and ω are nonzero and have the same sign, the choice $c = \omega/\tau > 0$ gives $\gamma = 0$. If we further choose $\phi = \pi/2$, then $u = [\tau \quad 0 \quad \kappa]^T$, and the frame R corresponds to the Frenet-Serret frame of the curve r.

We have shown that only three of the five parameters appearing in the expressions (4) are needed to determine the stability of a helical rod. We can therefore visualize the stability of all inextensible, unshearable, isotropic, and uniform helical rods within a three-dimensional parameter space with coordinates $\kappa > 0$, τ, and ω.

Star convexity of the stable subset.—We now derive a geometric property of the three-dimensional κ-τ-ω parameter space. Let $s_c(\kappa, \tau, \omega) > 0$ denote the first conjugate point along the helical rod with curvature $\kappa > 0$, torsion τ, and twisting moment ω, i.e., the first $s > 0$ at which $\det[J(s)] = 0$. If $s_c(\kappa, \tau, \omega) > L$, then the helical rod with length L, curvature $\kappa > 0$, torsion τ, and twisting moment ω is stable, whereas if $s_c(\kappa, \tau, \omega) < L$, then the helical rod is unstable. In the case $s_c(\kappa, \tau, \omega) = L$, the conjugate point test fails to give a definitive answer.

In the companion paper [36], we derive a scaling law that relates conjugate points along different helical rods. This scaling law states that for any choice of $\kappa > 0$, τ, and ω, and any positive number $\lambda > 0$, we have

$$s_c(\lambda\kappa, \lambda\tau, \lambda\omega) = \lambda^{-1} s_c(\kappa, \tau, \omega). \tag{6}$$

While this scaling law can be used to compare conjugate points along different helical rods, it also allows us to derive a geometric property of the subset of points in the κ-τ-ω parameter space that correspond to stable helical rods. Consider a rod of length L and suppose the point (κ, τ, ω) satisfies $s_c(\kappa, \tau, \omega) = L$. The point (κ, τ, ω) is on the boundary between stable and unstable helices. Next, for any $\lambda \in (0, 1)$ we have from (6) that $s_c(\lambda\kappa, \lambda\tau, \lambda\omega) > L$, and for any $\lambda > 1$ we have $s_c(\lambda\kappa, \lambda\tau, \lambda\omega) < L$. In other words, each ray extending from the origin in the κ-τ-ω parameter space intersects the boundary between stable and unstable helices at most once. Furthermore, we show in the companion paper [36] that for any (κ, τ, ω) with $\kappa > 0$, we have $s_c(\kappa, \tau, \omega) < \infty$, i.e., every helical rod becomes unstable at a finite length. We conclude that each ray extending from the origin in the κ-τ-ω parameter space intersects the boundary between stable and unstable helices exactly once.

This argument suggests that the subset of points in the κ-τ-ω parameter space corresponding to stable helical rods is star convex with respect to the origin. However, we must have $\kappa > 0$ for the conjugate point method to be applicable, and we therefore cannot have $\lambda = 0$. We conclude that the closure of the set of points corresponding to stable helical rods, which contains the origin, is star convex. This geometric property of stable helical rods would have been difficult to establish using exhaustive numerical computation in the κ-τ-ω parameter space.

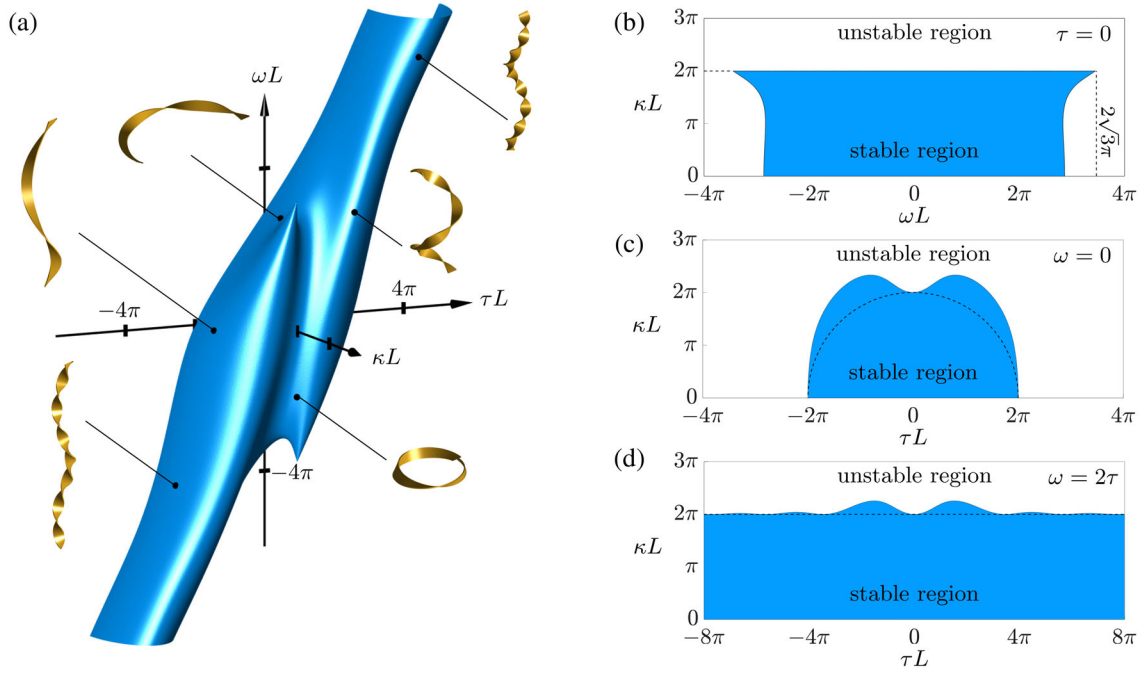

FIG. 2. The boundary between stable and unstable helical rods within the three-dimensional κL-τL-ωL parameter space. In Fig. 2(a), points within the surface correspond to stable helices, while points outside of the surface correspond to unstable helices. Also shown in Fig. 2(a) are six representative helical rods that lie on the surface. Although we consider isotropic rods, these representative helical rods are drawn as ribbons to show the rod's twist. Figures 2(b)–2(d) show planar sections of the surface in Fig. 2(a) corresponding to $\tau = 0$, $\omega = 0$, and $\omega = 2\tau$.

Computing the set of stable helices.—We now describe a method for computing the entire boundary between sets of stable and unstable helices in the κ-τ-ω parameter space. Consider a rod of length L, and pick a random point (κ, τ, ω) satisfying $\kappa > 0$. After computing $s_c(\kappa, \tau, \omega)$ and setting $\lambda = s_c(\kappa, \tau, \omega)/L$, we have from (6) that $s_c(\lambda\kappa, \lambda\tau, \lambda\omega) = L$. The point $(\lambda\kappa, \lambda\tau, \lambda\omega)$ is the unique intersection between the boundary and the ray that extends from the origin through the point (κ, τ, ω).

Using this method, the entire boundary separating stable and unstable helices for a rod of length L can be computed using the following steps: 1. Uniformly sample points on the hemisphere defined by $\sqrt{\kappa^2+\tau^2+\omega^2} = 2\pi$ and $\kappa > 0$. 2. For each point (κ, τ, ω) on the hemisphere, compute the first conjugate point $s_c(\kappa, \tau, \omega)$. 3. Let $\lambda = s_c(\kappa, \tau, \omega)/L$ and scale the point to obtain $(\lambda\kappa, \lambda\tau, \lambda\omega)$, which lies on the boundary.

Two examples of this procedure are shown in Fig. 1 with $L = 1$. In each example, the point (κ, τ, ω) is scaled by a factor of $s_c(\kappa, \tau, \omega)/L$ to obtain a point on the boundary. Note that varying the length L in the above steps simply changes the scaling factor λ. This dependence upon L can be removed by viewing the boundary between stable and unstable helical rods in a length-scaled parameter space with coordinates κL, τL, and ωL. Whereas each choice of L produces a different boundary in the κ-τ-ω parameter space, all of these boundaries collapse onto a single surface in the κL-τL-ωL parameter space.

Steps 1–3 were followed with $L = 1$ using 250 000 points on the hemisphere of radius 2π. For each point, the solution of (5) derived in the companion paper [36] was used to find $\det[J(s)]$, and the first conjugate point $s_c(\kappa, \tau, \omega)$ was found using numerical bisection in s. The resulting surface that separates stable and unstable helices within the κL-τL-ωL parameter space is shown in Fig. 2(a), along with six representative helices of length $L = 1$ that lie on the surface. Also shown in Figs. 2(b)–2(d) are three planar sections defined by $\tau = 0$, $\omega = 0$, and $\omega = 2\tau$. The surface is symmetric under $(\kappa, \tau, \omega) \to (\kappa, -\tau, -\omega)$, which corresponds to reversing both the helical rod's handedness and direction of twist.

Figure 2(b) corresponds to twisted circular rods, and the results in this figure agree with previous analysis of such rods. A closed circular rod (i.e., $\kappa L = 2\pi$) becomes unstable when $|\omega L| = 2\sqrt{3}\pi$ [at the cusps in Fig. 2(b)], a result first derived by Michell [39] [cf. [40], Eq. (11)]. Furthermore, in agreement with [27], p. 1373, multicovered circular rods with $\kappa L > 2\pi$ are unstable.

In Fig. 2(a), there appears to be a direction along which all helical rods with sufficiently small curvature are stable. As shown in Fig. 2(d), helical rods satisfying $\omega = 2\tau$ are stable if $\kappa < 2\pi/L$. Therefore, given any circular helix of length L with arbitrary torsion τ and with curvature κ satisfying $\kappa < 2\pi/L$, there exists a stable elastic rod of length L whose centerline traces the helix.

Conclusion.—Prior to this work, one of the only general descriptions of stability of all helical rods appeared in [6,7], and stated that a helical rod with clamped ends is stable if it is sufficiently short. In this Letter, we have computed the maximal length for all stable helical configurations of an inextensible, unshearable, isotropic, and uniform elastic rod. For given values of curvature, torsion, and twisting moment, the boundary in Fig. 2 can be used to determine this maximal length. These results relied on several invariance and scaling properties, and would have been difficult to obtain using exhaustive numerical computation. Our approach may lead to similar results for other models of thin elastic structures, such as anisotropic helical rods [5–7] and helical ribbons [41].

This work was supported by the NSF under Grant No. IIS-1320519. The work of A. B. was supported by the NSF-GRFP under Grant No. DGE-1144245 and by the NSF under Grant No. DMS-1645643.

*borum@cornell.edu
†tbretl@illinois.edu

[1] G. Kirchhoff, J. Reine Angew. Math. (Crelle) **56**, 285 (1859).
[2] A. E. H. Love, *A Treatise on the Mathematical Theory of Elasticity* (Dover, New York, 1944).
[3] S. S. Antman, Q. Appl. Math. **32**, 221 (1974).
[4] A. B. Whitman and C. N. DeSilva, J. Elast. **4**, 265 (1974).
[5] N. Chouaieb, Ph. D. thesis, Ecole Polytechnique Fédérale de Lausanne, Lausanne, Switzerland, EPFL thesis No. 2717, 2003.
[6] N. Chouaieb and J. H. Maddocks, J. Elast. **77**, 221 (2004).
[7] N. Chouaieb, A. Goriely, and J. H. Maddocks, Proc. Natl. Acad. Sci. U.S.A. **103**, 9398 (2006).
[8] A. Kumar and T. J. Healey, Comput. Methods Appl. Mech. Eng. **199**, 1805 (2010).
[9] A. Goriely and M. Tabor, Phys. Rev. Lett. **77**, 3537 (1996).
[10] A. Goriely and M. Tabor, Physica (Amsterdam) **105D**, 20 (1997).
[11] A. Goriely and M. Tabor, Physica (Amsterdam) **105D**, 45 (1997).
[12] A. Goriely and M. Tabor, Proc. R. Soc. A **453**, 2583 (1997).
[13] A. Goriely and M. Tabor, Proc. R. Soc. A **454**, 3183 (1998).
[14] A. Goriely and M. Tabor, Nonlinear Dyn. **21**, 101 (2000).
[15] A. Goriely and P. Shipman, Phys. Rev. E **61**, 4508 (2000).
[16] A. Goriely, M. Nizette, and M. Tabor, J. Nonlinear Sci. **11**, 3 (2001).
[17] S. Benoit, D. D. Holm, and V. Putkaradze, J. Phys. A **44**, 055201 (2011).
[18] Y.-Z. Liu and Y. Xue, J. Appl. Math. Mech. **32**, 603 (2011), English translation.
[19] Z. Zhou, P.-Y. Lai, and B. Joós, Phys. Rev. E **71**, 052801 (2005).
[20] Z. Zhou, Mod. Phys. Lett. B **19**, 249 (2005).
[21] Z. Zhou, B. Joós, P.-Y. Lai, Y.-S. Young, and J.-H. Jan, Mod. Phys. Lett. B **21**, 1895 (2007).
[22] Y.-C. Cheng, S.-T. Feng, and K. Hu, Math. Mech. Solids **22**, 2108 (2017).
[23] A. Majumdar and A. Raisch, Nonlinearity **27**, 2841 (2014).
[24] A. Majumdar and A. Goriely, Physica (Amsterdam) **253D**, 91 (2013).
[25] A. Majumdar, C. Prior, and A. Goriely, J. Elast. **109**, 75 (2012).
[26] R. S. Manning and K. A. Hoffman, J. Elast. **62**, 1 (2001).
[27] K. A. Hoffman, Proc. R. Soc. A **461**, 1357 (2005).
[28] J. M. T. Thompson and A. R. Champneys, Proc. R. Soc. A **452**, 117 (1996).
[29] K. A. Hoffman, Phil. Trans. R. Soc. A **362**, 1301 (2004).
[30] M. Cicalese, M. Ruf, and F. Solombrino, Calc. Var. **56**, 115 (2017).
[31] R. S. Manning, K. A. Rogers, and J. H. Maddocks, Proc. R. Soc. A **454**, 3047 (1998).
[32] K. A. Hoffman, R. S. Manning, and R. C. Paffenroth, SIAM J. Appl. Dyn. Syst. **1**, 115 (2002).
[33] S. S. Antman, *Nonlinear Problems of Elasticity*, 2nd ed. (Springer-Verlag, New York, 2005).
[34] R. Manning, SIAM Rev. **51**, 193 (2009).
[35] O. M. O'Reilly and D. M. Peters, J. Elast. **105**, 117 (2011).
[36] A. Borum and T. Bretl, companion paper, Phys. Rev. E **102**, 023004 (2020).
[37] T. Bretl and Z. McCarthy, Int. J. Robot. Res. **33**, 48 (2014).
[38] J. Biggs, W. Holderbaum, and V. Jurdjevic, IEEE Trans. Autom. Control **52**, 1027 (2007).
[39] J. H. Michell, Messenger Math. **11**, 181 (1889), https://rcin.org.pl/Content/108929/WA35_87310_cz294-1890-t19_Art11.pdf.
[40] A. Goriely, J. Elast. **84**, 281 (2006).
[41] E. L. Starostin and G. H. M. van der Heijden, Phys. Rev. Lett. **101**, 084301 (2008).